DOI: 10.1002/ejic.200700780

InN@SiO_2 Nanomaterials as New Blue Light Emitters

Prabhakaran Munusamy,[a] Venkataramanan Mahalingam,[a] and Frank C. J. M. van Veggel*[a]

Keywords: Hybrid nanomaterials / Blue photoluminescence / Indium nitride / Silica

In this article we report blue photoluminescence (≈ 450 nm) from InN@SiO_2 nanomaterials. The InN@SiO_2 nanomaterials were prepared by a simple precipitation reaction followed by a solid-state reaction. Various control experiments demonstrate that the interface between the InN and SiO_2 seems to play a crucial role in the origin of the blue emission from the InN@SiO_2 nanomaterial. The InN@SiO_2 nanomaterial was characterized by using analytical methods such as TEM, XRD, Raman, XPS, and photoluminescence spectroscopy, which confirmed the existence of InN on SiO_2 with a small excess of nitrogen relative to indium.

Introduction

There is an enormous focus of research on nanomaterials, especially semiconductor nanomaterials, because of their interesting physical and chemical properties.[1] Out of all semiconductors, group 13 nitride semiconductor materials are unique, as their optoelectronic properties can be exploited for the development of state-of-the-art electronic devices such as LEDs, displays, etc.[2] Among the group 13 nitrides, InN, though initially not having received much attention like GaN, is currently attracting more interest due to its excellent charge-carrier transport characteristics which are superior relative to two other nitride components, GaN and AlN.[3] In addition, other properties like saturation and steady-state drift velocities are higher for InN relative to its nitride counterparts.[3]

InN-based thin film studies are well-documented in the literature.[4] The optical properties of InN have attracted many scientists, as there exists a controversy over the location of their bandgap. Some groups report that the bandgap is in the NIR region,[5–7] whereas others report it in the visible region close to 1.8 eV (689 nm).[8,9] Here we focus on the studies reporting photoluminescence (PL) of InN-based materials in the visible region. Yodo et al. observed luminescence at 1.84 eV (674 nm) for InN layers grown on Si substrates by molecular beam epitaxy (MBE), which they assigned to donor-to-acceptor emission.[9] The same group reported band-edge emission close to 1.88 eV (659 nm) from InN films made with the electron-cyclotron-resonance-assisted MBE technique.[10] They also observed additional PL near 2.08 eV (596 nm) and 2.16 eV (576 nm), which they assigned to donor-bound excitation from α- and β-InN grains, respectively. InN epilayers grown by magnetron sputtering display visible PL near 1.9 eV (652 nm).[8]

Despite the large number of studies on InN-based thin films, research on synthetic routes to InN-based nanomaterials is quite limited.[11–13] Nanoparticle-based InN materials could be important for the cost-effective fabrication of large-area (flexible) light-emitting and display devices. Moreover, solution-based synthetic routes to InN would allow one to develop nanomaterials with different shapes and sizes.[14] For example, Sardar et al. developed a solvothermal route that produced nanowires and nanotubes along with nanocrystals of InN which exhibit PL near 675 nm.[13] Decomposition of the azide complex InN_3-$[CH_2CH_2CH_2NMe_2]_2$ in trioctylphosphane oxide results in the formation of 4.5-nm InN nanoparticles showing emission near 690 nm.[15] This emission at 690 nm is attributed to quantum confinement effects (assuming a bulk bandgap of 0.7 eV). Broad PL centered at 2.2 eV (563 nm) was observed from nanocrystalline InN by benzene thermal conversion of indium sulfide along with $NaNH_2$ as the nitrogen source.[16] Although most of these studies report PL in the red region, blue luminescence from InN-based materials are quite scarce. To the best of our knowledge, there are only two reports available.[14,17] Blue emission is interesting over other primary colors, as the optical data storage capacity increases roughly fourfold relative to that of the corresponding red counterpart.[18] Zhang et al. fabricated InN nanowire arrays that exhibit a broad, blue-green PL in the range 300–650 nm.[14] Deconvolution of the broad peak results in two peaks; the major peak is centered at 478 nm. This blue PL was attributed to the existence of defects such as indium or nitrogen vacancies (V_{In} or V_N) or to the presence of both. Recently, Liu and co-workers synthesized In-

[a] University of Victoria, Department of Chemistry,
P. O. Box 3065, Victoria, British Columbia V8W 3V6, Canada
E-mail: fvv@uvic.ca
Fax: +1-250-472-5193

O-N nanospheres, which display room-temperature cathodoluminescence (CL) centered at 454 nm.[17] This blue CL, which is redshifted relative to the blue PL from In_2O_3, is ascribed to nitrogen incorporation into indium oxide to form In-O-N moieties.

Here we report blue photoluminescence from an InN@SiO_2 nanomaterial, from which electroluminescence has recently been reported.[19] This material was prepared by following a synthetic strategy recently developed by us to grow semiconductor nanocrystals on silica nanoparticles[20] and is part of a larger effort to produce nanomaterials that show blue photo- and electroluminescence in polymer-based light-emitting diodes.[19–22] In fact, this work stimulated us to try other nitrides than GaN. Various control experiments show that the origin of the blue emission from this nanomaterial is most likely from the interface of InN and SiO_2. Complete characterization of the material was performed by using transmission electron microscopy (TEM), X-ray diffraction (XRD), photoluminescence (PL) measurements, X-ray photoelectron spectroscopy (XPS), and Raman spectroscopy.

Results and Discussion

The InN@SiO_2 nanomaterials were prepared by a simple precipitation followed by a solid-state reaction. The yellowish-white precursor hybrid nanomaterial, In_2O_3@SiO_2, was nitridated with ammonia, which resulted in the formation of a black material. The black color indicates the formation of InN. To understand the structure of the black material, TEM analysis was performed. The TEM image shown in Figure 1 (bottom) shows the formation of small nanostructures of InN that are attached to the surface of the silica particles, clearly not a core-shell structure. The TEM of the as-made SiO_2 beads is also presented in Figure 1 (top), clearly showing smooth surface before the surface modification. In order to confirm the formation of the InN we carried out an XRD analysis. Figure 2 shows the XRD pattern collected from the InN@SiO_2 nanomaterial. The peak assignments are indicated above the corresponding reflections. The observed pattern corresponds well to that reported for crystalline InN.[16] The broad diffraction peak at 20° (2θ) corresponds to the amorphous silica phase. Applying the Scherrer equation[23] to the line broadening of the InN peaks gives crystallite sizes in the range 5 to 10 nm, which is consistent with the features seen in Figure 1. Additionally, the formation of InN was confirmed by Raman spectroscopic analysis. Figure 3 displays the room-temperature Raman spectrum for InN@SiO_2 nanomaterial. The peak at a wavenumber of about 590 cm^{-1} is assigned to the A_1 [longitudinal optical (LO)] phonon peak of InN.[8,24] The characteristic Raman Si–O–Si bending vibration appearing at 430 cm^{-1} is not clearly seen in the spectrum, as it is overshadowed by the strong Raman band from InN.[25]

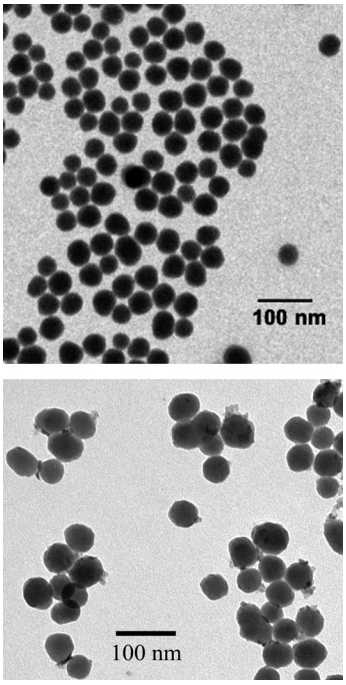

Figure 1. TEM images of as-made SiO_2 beads (top) and the InN@SiO_2 nanomaterial (bottom).

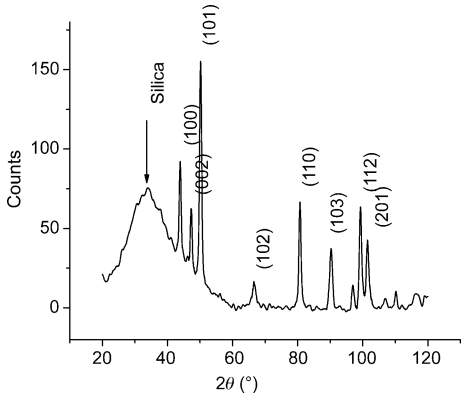

Figure 2. XRD pattern of the InN@SiO_2 nanomaterial.

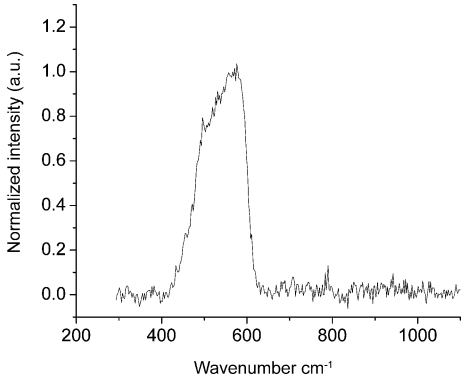

Figure 3. Raman spectrum of the InN@SiO_2 nanomaterial measured at room temperature.

Optical Properties of InN@SiO_2

The PL spectrum collected from InN@SiO_2 nanomaterial displays a blue emission centered at 450 nm as a result

of excitation in the UV region. This blue emission was easily seen by the naked eye. Figure 4A (left) shows the emission spectrum along with the excitation spectrum in the inset. The material has a strong absorption in the UV with a shoulder close to 275 nm and an onset at ≈ 300 nm. The emission peak is strongly blueshifted relative to the bandgap emission (600–700 nm) reported for InN nanomaterials. As quantum confinement effects are not expected in this case because of the irregular shapes of the nanomaterials, we performed various control experiments to understand the origin of the blue emission. First, to verify whether the emission was coming from the indium nitride, InN material alone was prepared by using similar procedure. No emission was observed from this sample. Second, the silica particles alone were heated in NH_3 under identical conditions. Only a very weak emission was observed from the SiO_2 after nitridation (Figure 4B). This weak emission could have come from carbon-related impurities present in silica, which has been observed earlier.[26–28] Thirdly, to confirm whether the emission is coming from the In_2O_3 that is present in a very small amount (In_2O_3 has broad emission in the blue region due to oxygen deficiencies),[29] and to understand the need for the nitridation, the precursor nanoparticles, i.e. In_2O_3@SiO_2 material was heated at 700 °C under an argon atmosphere. The absence of any characteristic emission from this sample (Figure 4C) indicates the importance of the presence of InN@SiO_2 in bringing about the blue emission. In order to confirm this, another control sample was made by mixing the In_2O_3, made by a similar procedure, and silica particles together followed by nitridation under the same conditions used for the preparation of InN@SiO_2. The resulting mixture displays only a very weak emission (Figure 4D), which highlights the importance of the InN growing on the surface of a SiO_2 nanostructure for the blue emission.

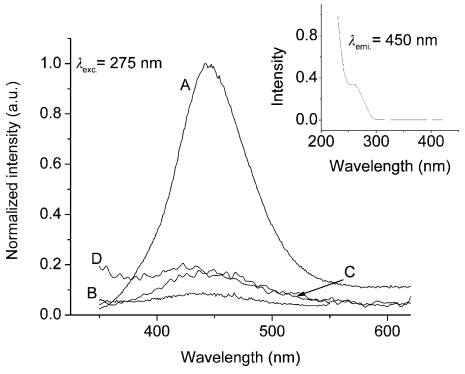

Figure 4. Emission spectrum of (A) the InN@SiO_2 nanomaterial, (B) bare silica particles after nitridation, (C) In_2O_3@SiO_2 heat treated in argon, and (D) In_2O_3 and SiO_2 mixed prior to nitridation. The inset shows the excitation spectrum collected from InN@SiO_2 nanomaterial. Spectra B, C, and D are multiplied by three for clarity.

The above control experiments clearly point to the importance of both InN and silica in bringing about the blue emission from InN@SiO_2 nanomaterial. Moreover, the near absence of any characteristic emission from the hybrid mixture (i.e. In_2O_3 and silica separately made and mixed together) after nitridation substantiates the importance of growing the In_2O_3 on the silica template (In_2O_3@SiO_2). This observation points to the fact that the interface between the InN and silica seems to play an important role in bringing about the blue emission. One possibility could be the formation of a different material such as $In_2Si_2O_7$ at the interface. Although $In_2Si_2O_7$ has characteristic luminescence, the luminescence mostly falls in the ultraviolet region.[30] Moreover, if the source of luminescence were $In_2Si_2O_7$, the precursor In_2O_3@SiO_2 would have exhibited the emission after being heated, but it only shows a weak emission (see above). The second possibility is the formation of an In-O-N complex as observed by Liu et al. in their In-O-N nanospheres.[17] The third possibility, which is closely related to second, is the widening of the optical bandgap of InN with the incorporation of oxygen.[31] This is reported for the polycrystalline InN where the bandgap was increased from 1.55 eV to 2.27 eV as the oxygen concentration was increased from 1% to 6%. We tentatively rule out these options, as we did not observe any bandgap emission in InN alone, made under identical conditions. To get more insight, XPS analysis was performed on the InN@SiO_2 as well on the precursor nanomaterials. The results indicate that for the precursor In_2O_3@SiO_2, the expected ratios of 1:1.5 and 1:2 were observed for In/O and Si/O, respectively. However, InN@SiO_2 an In/N ratio of 0.66 and a Si/O ratio of 1.98 were found. These results point towards the fact that the material is richer in N than strictly needed for InN. This indicates the formation of some sort of nitrogen-induced defects or formation of different phases such as oxynitrides particularly at the interface between InN and silica, which is the cause of the blue emission.

In principle the size of the InN, whether on the SiO_2 bead or separate, could matter for the blue emission, but the irregularity of the InN in the InN@SiO_2 hybrid material suggests that this is not the reason. Another possibility for the stronger blue emission of the InN@SiO_2 hybrid material is an energy transfer step from the excited InN to the SiO_2 followed by emission from a defect. For two reasons we believe this is not the case. The first is that shape of spectrum C and D and peak positions in Figure 4 are different from A. The second is that the mixture of InN and SiO_2 should have given a significantly higher emission than the other two controls (emissions B and C in Figure 4).

Conclusions

We have demonstrated the synthesis of a hybrid InN@SiO_2, which exhibits a blue emission when excited in the ultraviolet region. The structural characterization of the nanomaterials indicates formation of crystalline InN nanomaterial over the amorphous silica particles. Various control experiments support that the interface between the InN and silica plays an important role in the origin of the blue emission.

Experimental Section

Chemicals: Tetraethyl orthosilicate, aqueous ammonium hydroxide (28–30%), indium nitrate (99.98%), urea, potassium bromide, and ethanol (99.9%) were used as received from Aldrich. The anhydrous ammonia gas (99.999%) used for the nitridation was purchased from Praxair. Milli-Q water with a resistance greater than 18 MΩ was used in all our experiments.

Preparation of Monodisperse Silica Nanoparticles: The silica nanoparticles with an average size of 50 nm were synthesized by using a literature procedure.[32] Briefly, tetraethyl orthosilicate (3.8 mL) was added to a mixture containing ethanol (114 mL) and ammonium hydroxide (5.7 mL, 28–30%) with vigorous stirring. The stirring was continued overnight, which resulted in the formation of silica nanoparticles with average size of 50 nm. These silica particles were used as prepared, i.e. without isolation.

Preparation of the In_2O_3@SiO_2 Nanomaterial: This was prepared by adapting a procedure reported for Gd_2O_3:Eu@SiO_2.[33] Briefly, urea (0.6 g) dissolved in water (3 mL) was added to a flask containing 50-nm silica nanoparticles (15 mL). To this mixture, an aqueous solution of $In(NO_3)_3 \cdot xH_2O$ (1 mL, 0.2 M, $x = 5$, as provided by the supplier) was added dropwise. The resulting mixture was vigorously stirred at 85 °C for 3 h. The excess urea was removed by centrifugation and redispersion of the precipitate in water which was repeated three times. The resulting white product was dried in vacuo before being heated to 600 °C for 9 h.

Preparation of the InN@SiO_2 Nanomaterial: The In_2O_3@SiO_2 nanomaterial (approximately 100 mg) was taken in a quartz crucible and placed in an electric furnace (Lindberg HTF553222A with a CC58114PA controller). The furnace was heated to 700 °C at a rate of 5 °C per minute under an NH_3 atmosphere. The sample was kept at the final temperature for 2 h before it was cooled down to room temperature under an NH_3 atmosphere. The ammonia flow was maintained at 100 SCCM (cubic centimeter per minute at STP). The formation of InN was indicated by a color change of the sample from colorless to grayish black.

Photoluminescence Measurements: PL measurements were carried out by using an Edinburgh Instruments FLS 920 instrument with a 450 W Xe arc lamp and a red-sensitive Peltier element-cooled Hamamatsu R928 PMT. The measurement was done by using a solid sample holder. A KBr pellet was prepared by mixing the sample and the KBr in a weight ratio of 1:10 and placing the mixture in a solid sample holder. All spectra were recorded with 1 nm resolution and were corrected for the instrument response. The filters used were 320 nm and 435 nm for the collection of the emission and the excitation spectra, respectively.

X-Ray Powder Diffraction (XRD) Measurements: The XRD pattern of the InN@SiO_2 nanomaterial was collected by using a Rigaku Miniflex X-ray diffractometer with a Cr K_α (30 kV, 15 mA) radiation source. The nanoparticle samples were gently crushed to break down big lumps, and a thick paste was made with ethanol. This thick paste was evenly spread onto a clean quartz slide, and the ethanol was evaporated at 85 °C. The powder diffraction patterns were collected over the 2θ range 20 to 140° with a scan speed and sampling width of 1° min^{-1} and 0.02°, respectively.

Raman Spectroscopy: Raman spectra were collected by exciting the sample with 632.8 nm from a He-Ne Laser by Melles Griot. Roughly 20 mg of the solid sample was placed on a clean glass slide and spread evenly with a spatula. The spectrum is an average of 3 scans with a 30-s collection time for each scan.

Transmission Electron Microscopic Measurements: A Hitachi instrument with a H-7000 tungsten filament up to 125 kV was used to collect the TEM images. TEM specimens were prepared by dipping a copper grid (600 mesh) coated with an amorphous carbon film into the ethanol dispersion of the InN@SiO_2 nanomaterial and drying at room temperature.

X-Ray Photoelectron Spectroscopy: X-ray photoelectron spectra were collected by using a Leybold Max200 spectrometer equipped with a monochromatic Al-K_α X-ray source (1486.6 eV). The pass energy for the survey and narrow scans were 192 and 48 eV, respectively. Photoelectrons were collected at 90° from the surface. All binding energies (BE) were recorded relative to the C1s peak (BE: 285.0 eV).

Acknowledgments

Authors are grateful for the financial support received for this work from NSERC (Natural Sciences and Engineering Research Council of Canada) through the AGENO (Accelerator Grant for Exceptional New Opportunities) project, Canada Foundation for Innovation (CFI), and the British Columbia Knowledge Development Fund (BCKDF) of Canada.

[1] M. A. El-Sayed, *Acc. Chem. Res.* **2001**, *34*, 257.
[2] S. P. Denbaars, *Proc. IEEE* **1997**, *85*, 1740.
[3] A. G. Bhuiyan, A. Hashimoto, A. Yamamoto, *J. Appl. Phys.* **2003**, *94*, 2779.
[4] M. Nirmal, L. Brus, *Acc. Chem. Res.* **1999**, *32*, 407.
[5] T. Matsuoka, H. Okamoto, M. Nakao, H. Harima, E. Kurimoto, *Appl. Phys. Lett.* **2002**, *81*, 1246.
[6] T. Miyajima, Y. Kudo, K. L. Liu, T. Uruga, T. Honma, Y. Saito, M. Hori, Y. Nanishi, T. Kobayashi, S. Hirata, *Phys. Status Solidi B* **2002**, *234*, 801.
[7] Y. Saito, H. Harima, E. Kurimoto, T. Yamaguchi, N. Teraguchi, A. Suzuki, T. Araki, Y. Nanishi, *Phys. Status Solidi B* **2002**, *234*, 796.
[8] X. D. Pu, W. Z. Shen, Z. Q. Zhang, H. Ogawa, Q. X. Guo, *Appl. Phys. Lett.* **2006**, *88*, 151904.
[9] T. Yodo, H. Ando, D. Nosei, Y. Harada, *Phys. Status Solidi B* **2001**, *228*, 21.
[10] T. Yodo, H. Yona, H. Ando, D. Nosei, Y. Harada, *Appl. Phys. Lett.* **2002**, *80*, 968.
[11] K. Sardar, M. Dan, B. Schwenzer, C. N. R. Rao, *J. Mater. Chem.* **2005**, *15*, 2175.
[12] B. Schwenzer, L. Loeffler, R. Seshadri, S. Keller, F. F. Lange, S. P. DenBaars, U. K. Mishra, *J. Mater. Chem.* **2004**, *14*, 637.
[13] K. Sardar, F. L. Deepak, A. Govindaraj, M. M. Seikh, C. N. R. Rao, *Small* **2005**, *1*, 91.
[14] J. Zhang, B. L. Xu, F. H. Jiang, Y. D. Yang, J. P. Li, *Phys. Lett. A* **2005**, *337*, 121.
[15] P. S. Schofield, W. Z. Zhou, P. Wood, I. D. W. Samuel, D. J. Cole-Hamilton, *J. Mater. Chem.* **2004**, *14*, 3124.
[16] J. P. Xiao, Y. Xie, R. Tang, W. Luo, *Inorg. Chem.* **2003**, *42*, 107.
[17] B. Y. Liu, X. Y. Chen, J. L. Yao, *Nanotechnology* **2007**, *18*, 195604.
[18] S. P. Denbaars, *Proc. IEEE* **1997**, *85*, 1740.
[19] M. Tan, P. Munusamy, V. Mahalingam, F. C. J. M. Van Veggel, *J. Am. Chem. Soc.* **2007**, *129*, 14122.
[20] V. Mahalingam, M. Tan, P. Munusamy, J. B. Gilroy, F. C. J. M. van Veggel, *Adv. Funct. Mater.* **2008**, *18*, 9.
[21] V. Mahalingam, V. Sudarsan, P. Munusamy, F. C. J. M. van Veggel, R. Wang, A. J. Steckl, M. Raudsepp, *Small* **2008**, *4*, 105.
[22] M. Tan, V. Mahalingam, F. C. J. M. van Veggel, *Appl. Phys. Lett.* **2007**, *91*, 093132.
[23] J. C. Taylor, I. Hinczak, *Rietveld Made Easy*, Sietronics Pty Limited, Canberra (Australia), **2004**.
[24] C. H. Liang, L. C. Chen, J. S. Hwang, K. H. Chen, Y. T. Hung, Y. F. Chen, *Appl. Phys. Lett.* **2002**, *81*, 22.

[25] E. Berrier, C. Zoller, F. Beclin, S. Turrell, M. Bouazaoui, B. Capoen, *J. Phys. Chem. B* **2005**, *109*, 22799.
[26] L. T. Canham, A. Loni, P. D. J. Calcott, A. J. Simons, C. Reeves, M. R. Houlton, J. P. Newey, K. J. Nash, T. I. Cox, *Thin Solid Films* **1996**, *276*, 112.
[27] W. H. Green, K. P. Le, J. Grey, T. T. Au, M. J. Sailor, *Science* **1997**, *276*, 1826.
[28] J. Mu, L. H. Xu, X. B. Gao, Y. Y. Zhang, *J. Dispersion Sci. Technol.* **2005**, *26*, 483.
[29] C. H. Liang, G. W. Meng, Y. Lei, F. Phillipp, L. D. Zhang, *Adv. Mater.* **2001**, *13*, 1330.
[30] T. Gaewdang, J. P. Chaminade, P. Gravereau, A. Garcia, C. Fouassier, M. Pouchard, P. Hagenmuller, B. Jacquier, *Z. Anorg. Allg. Chem.* **1994**, *620*, 1965.
[31] M. Yoshimoto, H. Yamamoto, W. Huang, H. Harima, J. Saraie, A. Chayahara, Y. Horino, *Appl. Phys. Lett.* **2003**, *83*, 3480.
[32] H. Hiramatsu, F. E. Osterloh, *Langmuir* **2003**, *19*, 7003.
[33] G. X. Liu, G. Y. Hong, D. X. Sun, *J. Colloid Interface Sci.* **2004**, *278*, 133.

Received: July 23, 2007
Published Online: July 10, 2008

